Photorefractive keratectomy in the cat eye: Biological and optical outcomes

Lana J. Nagy, Scott MacRae, MD, Geunyoung Yoon, PhD,
Matthew Wyble, Jianhua Wang, PhD, Ian Cox, PhD, Krystel R. Huxlin, PhD

PURPOSE: To quantify optical and biomechanical properties of the feline cornea before and after photorefractive keratectomy (PRK) and assess the relative contribution of different biological factors to refractive outcome.

SETTING: Department of Ophthalmology, University of Rochester, Rochester, New York, USA.

METHODS: Adult cats had 6.0 diopter (D) myopic or 4.0 D hyperopic PRK over 6.0 or 8.0 mm optical zones (OZ). Preoperative and postoperative wavefront aberrations were measured, as were intraocular pressure (IOP), corneal hysteresis, the corneal resistance factor, axial length, corneal thickness, and radii of curvature. Finally, postmortem immunohistochemistry for vimentin and α-smooth muscle actin was performed.

RESULTS: Photorefractive keratectomy changed ocular defocus, increased higher-order aberrations, and induced myofibroblast differentiation in cats. However, the intended defocus corrections were only achieved with 8.0 mm OZs. Long-term flattening of the epithelial and stromal surfaces was noted after myopic, but not after hyperopic, PRK. The IOP was unaltered by PRK; however, corneal hysteresis and the corneal resistance factor decreased. Over the ensuing 6 months, ocular aberrations and the IOP remained stable, while central corneal thickness, corneal hysteresis, and the corneal resistance factor increased toward normal levels.

CONCLUSIONS: Cat corneas exhibited optical, histological, and biomechanical reactions to PRK that resembled those previously described in humans, especially when the OZ size was normalized to the total corneal area. However, cats exhibited significant stromal regeneration, causing a return to preoperative corneal thickness, corneal hysteresis and the corneal resistance factor without significant regression of optical changes induced by the surgery. Thus, the principal effects of laser refractive surgery on ocular wavefront aberrations can be achieved despite clear interspecies differences in corneal biology.

J Cataract Refract Surg 2007; 33:1051–1064 © 2007 ASCRS and ESCRS

Laser refractive surgery, a method that uses laser energy to ablate and reshape the corneal surface, has become an established form of vision correction. Although relatively successful at treating defocus and astigmatism, negative optical outcomes still occur. These include undercorrection, overcorrection, regression, and increases in the magnitude of higher-order optical aberrations (HOAs).[1] While the causes of such problems are clearly multifactorial, the biomechanical reaction of the cornea to the surgery is considered a major contributor to negative optical outcomes; in turn, corneal biomechanics are affected by several biological parameters such as corneal thickness, area, structural organization, molecular composition, and rigidity as well as by intraocular pressure (IOP)[2–4] (Yoon G-Y, et al. IOVS 2003; 44:E-Abstract 2029).

Most research into the effects of refractive surgery on ocular optics is performed in humans. This provides invaluable data, but is often limited ethically and practically by the needs of the patients. In turn, this limits our ability to properly assess the breadth and complexity of this surgery's effects on ocular optics and, especially, biology. Animal models such as rabbits, rodents, cats, and monkeys, which are traditionally used to study the biological consequences of laser refractive surgery, have taught us a lot about the wound-healing response of the cornea.[5–9] However, it has been difficult to correlate these biological changes with surgically induced changes in ocular optics. This is in part because most measures of ocular optical quality require steady fixation, which most animal models are not able to provide (Ramamirtham R, et al.

0886-3350/07/$—see front matter
doi:10.1016/j.jcrs.2007.02.021

IOVS 2003; 44:ARVO E-Abstract 1986; Ramamirtham R, et al. IOVS 2002; 43:ARVO E-Abstract 181; Coletta NJ, et al. IOVS 2003; 44:ARVO E-Abstract 1987; Kisilak ML, et al. IOVS 2003; 44:ARVO E-Abstract 4340). On the other hand, when anesthetized animals are used, there are significant alterations in tear film quantity and quality that negatively affect optical quality.[10]

An animal model was developed in which the problem of acquiring reliable measures of optical quality was overcome. Using established psychophysical methods,[11–14] normal adult cats were trained to repeatedly and precisely fixate on small visual targets on a computer screen while a compact Shack-Hartmann wavefront sensor was aligned to the line of sight and the pupillary center of each eye, as is done when measuring ocular wave aberrations in humans.[15] This allows accurate, reproducible measurements of ocular wave aberrations at multiple time points before and after laser refractive surgery in the awake, fixating, normally blinking state. Using this paradigm, it was recently shown[15] that the optical quality of the unoperated adult cat eye is as good as that of the normal adult human eye. Aside from its excellent optical quality, several other factors make the cat eye an excellent model for refractive surgery research. Cat corneas are by no means identical to human corneas. For instance, they have greater diameters than human corneas.[16–20] However, some of the cat corneal parameters most likely to affect corneal biomechanical properties (thickness, cellular and structural organization, molecular composition) closely approximate those of the human cornea.[20–26] This is a critical point because the cornea is the ocular structure that contributes to most of the power of the eye[27] and of the HOAs induced after laser refractive surgery.[28,29] Although rabbits are often the animal model of choice in refractive surgery research, cats have also been used successfully in studies of corneal wound healing after refractive procedures.[7,30,31] By adding the ability to reliably quantify optical wave aberrations to the repertoire of experimental manipulations that can be performed in cats, we are now in a stronger position to correlate optical, biomechanical, and biological outcomes of ophthalmological interventions in a single animal model. Such studies are critical if we are to understand the biological and biomechanical substrates of negative optical outcomes after manipulations of the ocular surface.

The goals of the present study were to use the awake, fixating cat animal model to (1) quantify optical and biomechanical properties of intact cat corneas; (2) assess the effect of photorefractive keratectomy (PRK), a form of laser refractive surgery, on the optical, biological, and biomechanical properties of cat corneas in situ; and (3) assess the relative contribution of different biomechanical factors, in particular corneal area and native corneal rigidity, in attaining optimum refractive outcomes after PRK.

MATERIALS AND METHODS

Subjects

Data were obtained from 26 eyes of 14 normal male domestic shorthair cats (*felis cattus*). Two eyes of 1 animal were eliminated from analysis because of postoperative complications (persistent inflammation and development of corneal sequestra). All cat procedures were conducted in accordance with the guidelines of the University of Rochester Committee on Animal Research, the ARVO Statement for the Use of Animals in Ophthalmic and Vision Research, and the NIH Guide for the Care and Use of Laboratory Animals. Corneal viscoelastic properties and IOP were measured in 16 eyes of 8 young adult human subjects, none of whom had refractive surgery or exhibited ocular pathologies. Axial lengths were also measured in 12 eyes of 6 of these subjects. All human measurements (axial length, corneal hysteresis, corneal resistance factor, and IOP) were conducted after the administration of informed consent

Accepted for publication February 12, 2007.

From the Department of Ophthalmology (Nagy, MacRae, Yoon, Wyble, Wang, Huxlin), University of Rochester, and Bausch & Lomb (Cox), Rochester, New York, USA.

Drs. MacRae and Yoon have served as consultants to Bausch & Lomb. Dr. Cox is a full-time employee of Bausch & Lomb. The University of Rochester has a research contract with Bausch & Lomb and has licensed intellectual property to them. No other author has a financial or proprietary interest in any material or product mentioned.

Supported by National Eye Institute grant RO1 EY015836-01, a grant from Bausch & Lomb Inc. to the University of Rochester's Center for Visual Science, grants from the University of Rochester's Center for Electronic Imaging Systems, a NYSTAR-designated Center for Advanced Technology, and by an unrestricted grant to the University of Rochester's Department of Ophthalmology from the Research to Prevent Blindness Foundation, New York, New York, USA.

Margaret Beha trained and tested the cats and did the feline ocular response analyzer (ORA) measurements. John Swanstone provided programming expertise. Tracy Bubel did the histological processing of the cat corneal tissue and hematoxylin staining. Emily Brandon, Shawn Kenner, and Sally Jensen analyzed the spot array patterns. Terry Schaeffer did the IOLMaster measurements. David Luce, PhD, provided access to the Reichert ORA. Gary Gagarinas assisted in laser refractive surgeries. Jens Bühren, MD, provided constructive discussions and feedback on the manuscript.

Corresponding author: Krystel Huxlin, PhD, Department of Ophthalmology, Box 314, University of Rochester Medical Center, 601 Elmwood Avenue, Rochester, New York 14642, USA. E-mail: huxlin@cvs.rochester.edu.

and in strict adherence to the tenets of the Declaration of Helsinki.

Ocular Wave Aberrations in Awake-Fixating Cats

Cats were trained using standard psychophysical methods.[11,15] Briefly, each cat was placed inside a magnetic field driven by 50 cm coils and its head was immobilized using an implanted cranial post. Electrical signals from an implanted subconjunctival eye coil were captured and calibrated using an eye-coil phase detector (Riverbend Electronics). The animals were trained to fixate on small (0.03 degree visual angle) spots of light on a dark 19-inch ViewSonic PF790 computer monitor 48 cm from their eyes. They were rewarded for maintaining their gaze within an electronically defined, 1-degree square window around each fixation spot and trained until they could maintain steady fixation within this window for 2.5 to 5 seconds. A compact Shack-Hartmann wavefront sensor was placed on a height-adjustable platform between the cat and the computer monitor.[15] An infrared pupil camera was used to align the wavefront sensor to the pupillary center of 1 eye, while the other eye fixated on a spot on the computer monitor.[15] Spot array patterns were collected preoperatively and 1, 3, and 6 months after PRK. Wave aberrations were calculated from the spot arrays using the Zernike polynomial expansion up to the 10th order. Only data pertaining to the 2nd to 5th orders (j = 3 to 20) are presented because they are most significant for visual performance. The amplitude (micrometers) of individual Zernike terms was calculated for the largest pupil diameter that could be obtained (usually 8.0 to 9.0 mm); MatLab (MathWorks) was used to derive their corresponding amplitude for a 6.0 mm diameter aperture, in agreement with the Optical Society of America standards.[32] The accuracy of this renormalization of the Zernike coefficients was verified by analyzing spot array patterns over a 6.0 mm pupillary aperture and comparing the aberrations measured with those calculated by interpolation from a 9.0 mm aperture. There was no significant difference between these 2 methods for any Zernike coefficient values up to j = 20. The magnitude of the defocus terms (Z_2^0, j = 4) was converted to diopters (D) using the formula:

$$D = \frac{-4\sqrt{3}Z_2^0}{(r)^2}$$

where r = radius (millimeters) of the analysis pupil. The total root mean square (RMS) of j = 3 to 20 and the higher-order RMS for j = 6 to 20 were also calculated as described previously.[15]

Corneal Thickness and Radii of Curvature

Optical coherence tomography (OCT) was used to image the cornea across the nasal–temporal meridian both before and 1, 3, and 6 months after PRK in the 4 cat eyes that had ablations over 8.0 mm optical zones (OZs). This resulted in 2 eyes with hyperopic and 2 eyes with myopic corrections. For the OCT imaging, the animals were first anesthetized with a mixture of ketamine and xylazine (5 mg/kg and 1 mg/kg, respectively), after which a drop of hydroxypropyl methylcellulose–sodium perborate eye gel (GenTeal) was administered to each eye. The anesthetized cats were placed in a custom-made head-restraint device to hold their head stable for imaging. A custom-made anterior segment OCT[33,34] was aligned to the apex of each cornea. Using a 1310 nm scanning laser, the OCT recorded a video stream of the cornea at a rate of 8 frames per second, as previously reported.[33,34] A mean normalized profile of backscatter light intensity over the central 105 μm of each cornea was generated from 25 corneal images isolated from the video stream. In each intensity profile, a peak or maximum amplitude of light reflectivity, corresponding to an interface between 2 different layers, was used to obtain the epithelial, stromal, and total corneal thicknesses.[33,34] The same OCT images were used to calculate corneal surface curvatures. After scaling to correct for optical distortion of each image, a custom edge-detection algorithm was used to select pixels within a user-defined zone that encompassed the epithelial–tear film (plus gel) interface, epithelial–stromal interface, or stromal–endothelial interface. The software then fitted a best-fit sphere to each interface and determined its radius of curvature over the central 6.0 mm of the cornea (for epithelial and stromal surfaces) and the central 5.0 mm of cornea (for the endothelial surface). Photorefractive keratectomy–induced changes in these 3 radii of curvature were then calculated and their absolute values computed 1, 3, and 6 months after PRK.

Intraoperative ultrasonic pachymetry was performed to obtain an estimate of the amount of stromal tissue removed during PRK. Five to 10 readings were collected at the center and the inner edge of a 6.0 or 8.0 mm marking ring using a Corneo-Gage Plus 2 ultrasonic pachymeter (Sonogage) immediately before and immediately after PRK over 6.0 or 8.0 mm OZs, respectively. Central thickness measurements were important in assessing how much tissue had been removed in myopic PRK, during which most tissue removal occurs in the center of the ablation. However, in hyperopic PRK, most tissue removed is at the ablation periphery; it is at this "trough" that peripheral measurements of corneal thickness were performed with the ultrasonic pachymeter. The preoperative total central corneal thickness (CCT) values collected with the Sonogage pachymeter were not significantly different from those obtained by OCT in the same animals (data not shown).

Ocular Axial Length

To exclude the possibility that small refractive changes observed after PRK in cats might be the result of an aggressive emmetropization process, partial coherence interferometry with the IOLMaster (Zeiss) was used to measure ocular axial length preoperatively and 1 and 3 months after PRK. The cats were anesthetized and positioned in a head-holding device with their head facing forward. The nictitating membranes were retracted with phenylephrine hydrochloride 2.5% drops, and the eyes were blinked manually to preserve surface quality. The IOLMaster was aligned according to standard procedures, and 5 measurements were collected per eye. Similar measurements were performed in 12 eyes of 6 human subjects whose heads were stabilized using a chin–forehead rest. They were asked to fixate on the instrument's red target light while 5 measurements were collected from each eye.

Intraocular Pressure, Corneal Hysteresis, and Corneal Resistance Factor Measurements

For cats, these measurements were collected in the anesthetized state. GenTeal eye gel was used to preserve corneal

hydration. An ocular response analyzer (ORA) (Reichert) was automatically aligned to the center of each eye and 5 or 6 measurements of corneal hysteresis, the corneal resistance factor, Goldmann-like IOP (IOPg), and cornea-compensated IOP (IOPcc) were collected[2] (Luce DA. IOVS 2006; 47:ARVO E-Abstract 2266). For human measurements, the subjects first applied a drop of GenTeal eye gel to each eye to replicate conditions under which data were collected in the cats. They sat with their heads resting in the machine's chin–forehead rest and were asked to fixate on the instrument's green target while 5 or 6 measurements were collected from each eye.

The experimental setup provided an excellent opportunity to assess the repeatability of measurements collected using the ORA in a cat animal model, comparing them with repeatability of the same instrument in human subjects. To this effect, the coefficients of variation for measurements of corneal hysteresis, corneal resistance factor, IOPg, and IOPcc were computed in the sample of cats (preoperatively) and in normal human eyes. In all cases, the coefficient of variation was calculated by dividing the standard deviation of the mean obtained from each measurement session (consisting of 5 or 6 measurements) by the mean value obtained during that session. The coefficient of variation was then expressed as a percentage of the mean for each measurement type and session. The lower the coefficient of variation, the more repeatable the measurements obtained with the ORA.

Photorefractive Keratectomy

Five cat eyes had 6.0 D myopic PRK, 3 over 6.0 mm OZs and 2 over 8.0 mm OZs. The OZ was defined as a "true" OZ, not including the transition zone that was present in every ablation type. Another 5 eyes had 4.0 D hyperopic PRK, 3 over 6.0 mm OZs, and 2 over 8.0 mm OZs. All procedures were conventional spherical ablations with transition zones. They were performed with the cats under surgical anesthesia using a Technolas 217 laser (Bausch & Lomb). Preoperatively, the corneas were treated with proparacaine hydrochloride 0.5% and the nictitating membrane was retracted with phenylephrine hydrochloride 2.5%. The eyes were stabilized with temporary sutures placed on the inferior and superior portions of the conjunctiva and attached using a 2-inch mosquito clamp to the cheek skin or brow. Before the actual ablation, each eye was marked with a blue 6.0 or 8.0 mm ring centered on the dilated pupil. Pachymetry was performed as described above. The epithelium was then scraped off, and measurements of stromal thickness were performed as described earlier. The difference between the pachymetry before and after scraping yielded the approximate central epithelial thickness in each cat eye. After surgery, ultrasonic pachymetry was repeated to estimate the amount of tissue removed by the ablation. The cornea was not irrigated after removal of the epithelium to minimize swelling that would result from such hydration. After surgery, the cats received 2 drops of tobramycin and dexamethasone (TobraDex) per eye, which was continued once per day until the surface epithelium healed (approximately 1 week postoperatively).

Postmortem Histology

Six cats had 6.0 D myopic PRK over 6.0 mm OZs for the purpose of obtaining postmortem histopathology. Three cats were killed 1 month postoperatively, and another 3 cats were killed 3 months after PRK. Cats were anesthetized with a mixture of ketamine and xylazine (5 mg/kg and 1 mg/kg, respectively) before receiving an overdose of sodium pentobarbital (100 mg/kg). Once all reflexes had disappeared, the corneas were excised and drop-fixed in a solution of 1% paraformaldehyde in 0.1 M phosphate-buffered saline (PBS), pH 7.4, for 10 minutes, after which they were transferred to a solution of 30% sucrose in 0.1 M PBS, and stored at 4°C for 2 days. Once suitably cryoprotected, the corneas were embedded in Tissue Tek OCT compound (Sakura Finetek) and 20 μm thick serial sagittal sections were cut on a cryostat. The sections were collected on microscope slides and stored in a −20°C freezer until ready to stain.

A set of sections from each cornea was stained with hematoxylin according to routine protocols. Adjacent sets were stained with antibodies against vimentin to label corneal keratocytes or α-smooth muscle actin (α-SMA) to label myofibroblasts. The immunoreactions were performed in a humidified chamber at room temperature. Sections were first incubated with primary antibodies: monoclonal mouse anti-vimentin (Clone V9 used at 1:100; sigma) or monoclonal mouse anti–α-SMA (used at 1:50) overnight. They were rinsed with 0.1 M PBS and incubated for 4 hours with biotinylated secondary antibodies (Vectastain ABC Elite Kit). After further rinsing, the sections were incubated with ABC reagent (Vectastain ABC Elite Kit) for 1 hour. After another set of rinses, they were incubated with 0.5% diaminobenzidine (DAB) in 0.1 M PBS in the presence of hydrogen peroxide to generate a permanent, brown product. After a final set of rinses, the sections were dehydrated, cover-slipped, and examined using an Olympus AX70 microscope. All photomicrographs presented in the Results section were collected via a high-resolution, high-sensitivity video camera interfaced with a personal computer running Image-Pro software (Media Cybernetics). Image-Pro was used to capture images, which were then transferred to Microsoft PowerPoint for assembly and labeling.

Statistical Analysis

Mean values in the groups were compared using the 2-tailed unpaired Student *t* test. A *P* value less than 0.05 was considered statistically significant. Changes in defocus, higher-order RMS, and corneal radii of curvature induced by myopic or hyperopic PRK over 6.0 or 8.0 mm OZs between 1 and 6 months postoperatively were tested with a mixed-factorial analysis of variance (ANOVA), with group (ie, 6.0 mm OZ versus 8.0 mm OZ or myopic PRK versus hyperopic PRK) as between-subject factors and postoperative time as the repeated measure. In all cases, a *P* value less than 0.05 was considered significant.

RESULTS

Preoperative Ocular Biometry

Table 1 compares cat biometric values measured in this study and human biometric values, some measured in this study and others collected from the literature. This comparison revealed some similarities and several significant differences between cat corneas and human corneas. Cat IOPcc and human IOPcc were not significantly different. In addition, the total and epithelial thicknesses of the central cat cornea were

Table 1. Comparison of native cat and human ocular biometrics.

Parameter	Mean ± SD	
	Cat	Human
Corneal thickness (µm)	575 ± 53	552 ± 32†
Epithelial thickness (µm)	54.0 ± 20.3	50.6 ± 3.9†
IOPg (mm Hg)*	12.3 ± 4.5	15.7 ± 2.9
IOPcc (mm Hg)	16.0 ± 5.4	14.8 ± 3.7
Corneal hysteresis (mm Hg)*	7.9 ± 2.0	11.1 ± 0.8
Corneal resistance factor (mm Hg)*	6.2 ± 1.5	10.0 ± 0.9

IOPcc = cornea-compensated IOP; IOPg = Goldmann-like IOP
*Significant difference between cat and human values ($P \leq .05$, Student *t* test)
†Values for human subjects not measured in the present study but obtained from Li HF, Petroll WM, Møller-Pedersen T, et al. Epithelial and corneal thickness measurements by in vivo confocal microscopy through focusing (CMTF). Curr Eye Res 1997; 16:214–221

within the normal range reported for humans. However, axial length, corneal hysteresis, IOPg, and the corneal resistance factor were all significantly smaller in cats than in humans ($P < .05$, 2-tailed Student *t* test).

The calculation based on measurements collected with the ORA in cats and humans found that the coefficients of variations for corneal hysteresis, corneal resistance factor, and IOPg were significantly smaller in humans than in cats. The mean corneal hysteresis coefficient of variation was 7.9% ± 5% (SD) in humans and 16.3% ± 9% in cats ($P < .05$, 2-tailed Student *t* test). The coefficient of variation for the corneal resistance factor measurements was 6.8% ± 4.9% in humans and 18.4% ± 9.4% in cats and for IOPg, 7.5% ± 3.5% and 12.0% ± 5.4%, respectively (both $P < .05$, 2-tailed Student *t* test). However, the coefficient of variation for IOPcc measurements was not statistically different between the 2 species (12.6% ± 8.2% for cats and 14.0% ± 8.2% for humans) ($P > .05$, 2-tailed Student *t* test). However, in all cases in which a significant difference was observed between mean ORA measurements collected in cats and humans (IOPg, corneal hysteresis, and the corneal resistance factor), the difference (28% for IOPg, 41% for corneal hysteresis, and 61% for the corneal resistance factor) was significantly larger than the coefficient of variation for that measurement in either species.

Preoperative Optical Aberrations

The sample of preoperative cat eyes showed excellent optical quality. The magnitude of lower-order and higher-order wavefront aberrations was small (Figure 1, *C* and *D*), with a mean total RMS of 1.27 ± 0.66 µm. The mean higher-order RMS was 0.41 ± 0.24 µm, representing 10.3% of the variance of the total RMS.

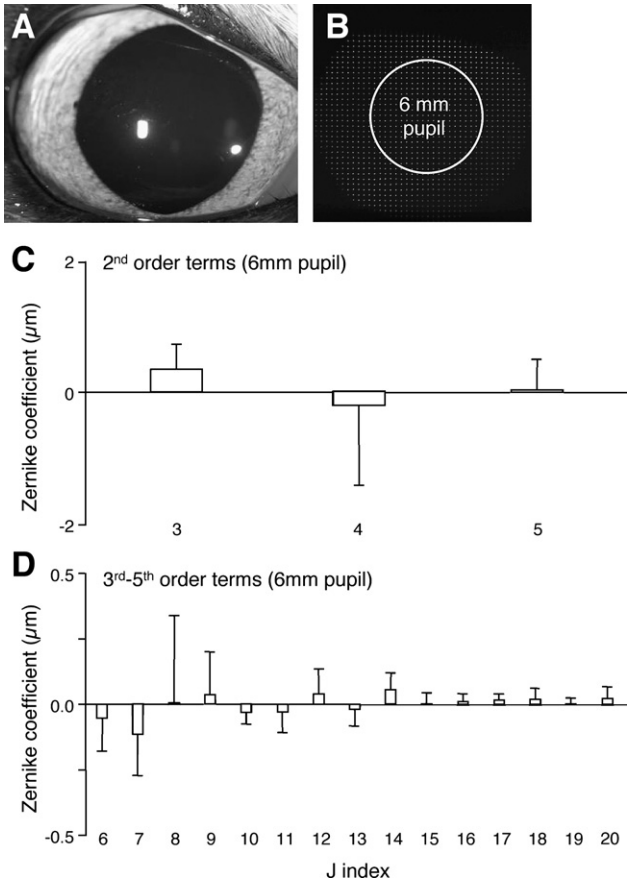

Figure 1. Wavefront aberrations in the normal cat eye. *A*: Photograph of a preoperative feline eye. *B*: Sample feline spot array pattern collected in the awake-behaving state using a modified Shack-Hartmann wavefront sensor. Note that the shadow created over the spot array pattern by the upper eyelid is well beyond the 6.0 mm analysis pupil used to measure wave aberrations. *C*: Preoperative lower-order wave aberrations for the 10 cats that had PRK. Note the small magnitude of lower-order aberrations, including defocus (j = 4) and the 2 astigmatism terms (j = 3 and 5). *D*: Preoperative Zernike coefficient values for HOAs (up to 5th-order Zernike coefficients, j = 20) were also relatively low. Note the small amount of spherical aberration (j = 12) in the sample of cat eyes (values expressed as means ± SD).

Effect of Photorefractive Keratectomy on Optical Aberrations

Six Millimeter Optical Zone Laser refractive surgery over 6.0 mm OZs in cats induced significant hyperopic shifts (after myopic PRK) and myopic shifts (after hyperopic PRK) in their defocus term (j = 4) relative to preoperative values (Figure 2). However, 1 month after surgery, only a mean of 2.2 ± 0.4 D and −0.8 ± 1.2 D of defocus change was observed after

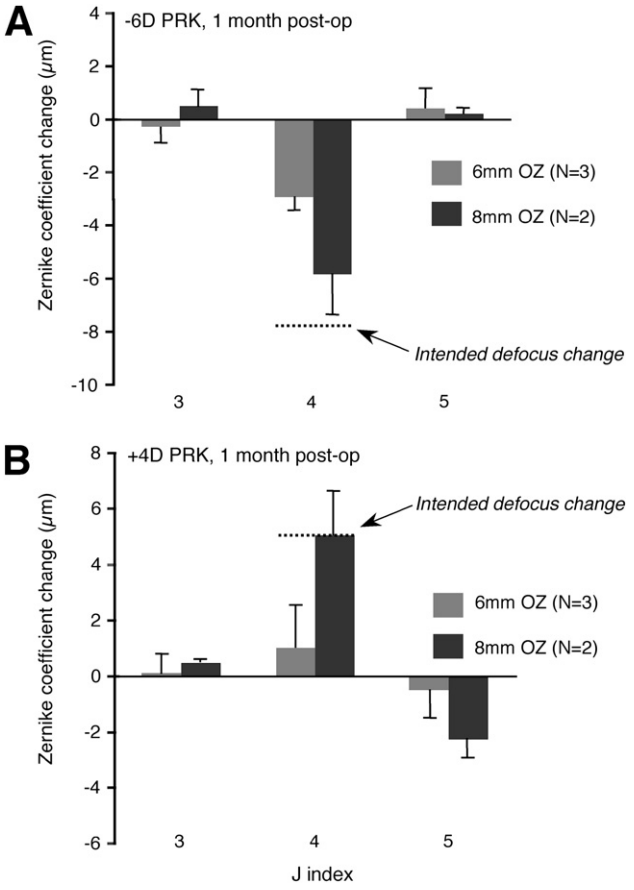

Figure 2. Change in the magnitude of lower-order wavefront aberrations (j indices 3 to 5) between preoperative values and values 1 month after myopic PRK (*A*) and hyperopic PRK (*B*) in the cat. Note the significantly lower magnitude of defocus change (j = 4) achieved by ablations over 6.0 versus 8.0 mm OZs. Defocus values for 6.0 mm OZs were well below the intended defocus change (dotted line). No significant differences were observed for the amount of astigmatism change induced by either type of surgery (values expressed as means ± SD; N = number of eyes treated in each group).

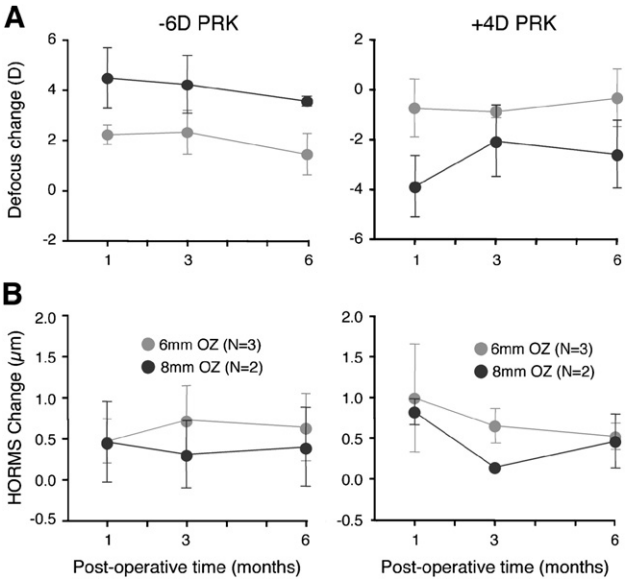

Figure 3. Stability of refractive changes induced over a 6-month period by PRK over 6.0 or 8.0 mm OZs in the cat. *A*: No significant differences were observed between 1 month and 6 months in any of the experimental groups with respect to dioptric change in the defocus term from preoperative values for −6.0 D myopic PRK or +4.0 D hyperopic PRK. *B*: Higher-order RMS change from preoperative values also showed no significant regression between 1 month and 6 months after PRK (values expressed as means ± SD; N = number of eyes treated in each group).

−6.0 D myopic ablations and +4.0 D hyperopic ablations, respectively (Figure 2). The amount of astigmatism (j = 3 and 5) induced was relatively small in all cases (Figure 2); however, HOA increased significantly (Figure 3). When myopic and hyperopic ablations 1 month postoperatively were grouped, the higher-order RMS increased by a mean of 0.78 ± 0.51 μm relative to preoperative values ($P < .05$, 2-tailed Student *t* test), representing approximately 32% of the variance of the total RMS. Most of this increase was the result of 3rd-order aberrations, especially vertical coma (j = 7), which increased by a mean of 0.29 ± 0.82 μm relative to preoperative values (Figure 3). Spherical aberration (j = 12) became more positive by a mean of 0.18 ± 0.20 μm after myopic treatments and more negative by a mean of 0.47 ± 0.61 μm after hyperopic treatments (Figure 3). An ANOVA showed that between 1 month and 6 months after PRK over a 6.0 mm OZ, cats showed no significant changes in defocus ($P = .206$ for myopic PRK; $P = .06$ for hyperopic PRK (Figure 4) or higher-order RMS ($P = .678$ for myopic PRK; $P = .257$ for hyperopic PRK) (Figure 3, *B*).

Eight Millimeter Optical Zone One month after PRK over an 8.0 mm OZ, cats had a mean 4.5 ± 1.2 D hyperopic shift (after 6.0 D myopic PRK) and a mean −4.2 D ± 1.6 D myopic shift (after 4.0 D hyperopic PRK) (Figures 2 and 4), which showed no statistically significant changes over the ensuing 5 months ($P = .206$ for myopic PRK and $P = .06$ for hyperopic PRK, ANOVA) (Figure 4, *A*). However, the same ANOVA found a significant effect of OZ size on defocus change after myopic PRK that resulted in consistently greater changes in defocus from preoperative levels in 8.0 mm OZs compared with 6.0 mm OZs ($P = .028$). The ANOVA showed this to be true at all time points examined. For hyperopic PRK, the ANOVA found no significant effect of OZ size but a significant interaction between OZ size and postoperative time ($P = .048$), which suggests the existence of slightly different temporal trends for 4.0 D hyperopic ablations over 6.0 mm OZs versus 8.0 mm OZs. Figure 4, *A*, shows the greater temporal variability in the defocus term for 4.0 D

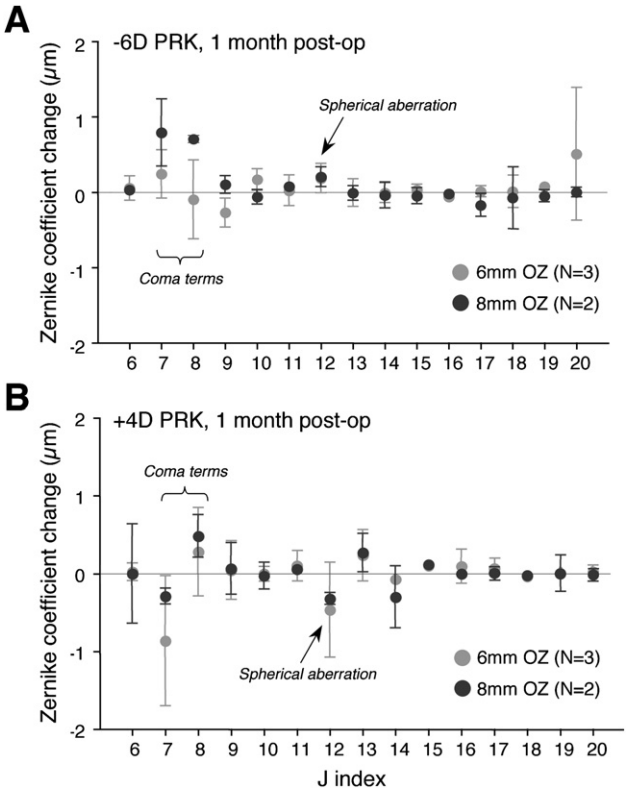

Figure 4. Change in the magnitude of higher-order wavefront aberrations (j indices 6 to 20) between preoperative values and values 1 month after myopic PRK (*A*) and hyperopic PRK (*B*) in the cat. No systematic differences were observed between changes induced over 6.0 or 8.0 mm OZs after either −6.0 D myopic PRK or +4.0 D hyperopic PRK. Spherical aberration (j = 12) increased in the positive direction after myopic PRK and in the negative direction after hyperopic PRK, regardless of OZ size. The magnitude of vertical and horizontal coma terms (j = 7 and 8 respectively) increased, but this was not consistently related to the OZ size (values expressed as means ± SD; N = number of eyes treated in each group).

hyperopic ablations over 8.0 mm OZs compared with the same ablations performed over 6.0 mm OZs.

The higher-order RMS induced by PRK over 8.0 mm OZs showed no main effect of OZ size over the 6 months after the surgery ($P = .580$ for myopic PRK; $P = .306$ for hyperopic PRK; ANOVA) and no significant interaction between OZ size and postoperative time ($P = .056$ for myopic PRK; $P = .564$ for hyperopic PRK; ANOVA). The mean higher-order RMS increased relative to preoperative values was 0.64 ± 0.36 μm; however, this represented only approximately 15% of the total variance in RMS 1 month after PRK. Most of the increase in higher-order RMS was again the result of increases in coma terms (j = 7 and 8), while spherical aberration (j = 12) changed relatively little (mean +0.20 ± 0.13 μm after myopic PRK and –0.32 ± 0.08 μm after hyperopic PRK (Figure 3). Overall, the higher-order RMS did not change significantly from 1 to 6 months postoperatively ($P = .444$ for myopic PRK; $P = .257$ for hyperopic PRK; ANOVA (Figure 4, *B*), although that this lack of significance may the result of the small sample size cannot be excluded.

Effect of Photorefractive Keratectomy on Ocular Biometry

Photorefractive keratectomy removed similar amounts of corneal stroma in cats as predicted by the Technolas laser algorithm, which is based on the instrument's performance in humans. For cat ablations over 6.0 mm OZs, the laser removed a mean of 72 ± 28 μm of stromal tissue as assessed from intraoperative pachymetry. As indicated earlier, this value was computed from pachymetry measurements collected at the deepest parts of the myopic and hyperopic ablations: centrally for myopic ablations and just inside the ablation zone for hyperopic ablations. The amount of tissue actually removed by the 6.0 mm ablations in cats was not significantly different ($P = .1$, 2-tailed Student *t* test) from the depth of removal (mean 91 ± 14 μm) predicted for these ablations by the Technolas 217Z laser's technical documentation (Bausch & Lomb). However, the 8.0 mm OZ ablations yielded significantly less tissue removal than predicted by the laser algorithm; only a mean of 110 ± 22 μm of stromal tissue was removed compared with the predicted 172 ± 20 μm ($P < .05$, 2-tailed Student *t* test).

Because only corneas that received PRK over 8.0 mm OZs attained close to intended refractive corrections, they were selected for OCT imaging to examine the rate of remodeling of the different corneal layers (ie, epithelium versus stroma) and changes in the curvature of the epithelial, stromal, and endothelial surfaces. The OCT measurements of the 4 cat corneas that had myopic ablations (n = 2) and hyperopic ablations (n = 2) over 8.0 mm OZs (Figure 5, *A* and *B*) showed that as expected, significantly more stromal tissue was removed from the central cornea in myopic treatments than in hyperopic treatments. By 1 month after myopic PRK, stromal, epithelial, and hence total, thickness of the central cornea had returned to normal levels, remaining stable over the ensuing 5 months (Figure 5, *A*). Cats that had hyperopic treatments also had a return to normal in central stromal and epithelial thicknesses, although the return appeared to be more gradual than after myopic PRK, with changes still occurring 6 months after PRK (Figure 5, *B*).

After 8.0 mm myopic PRK, the radius of curvature of the central 6.0 mm of the epithelial surface increased from a mean of 8.96 ± 0.9 mm preoperatively to a mean of 9.74 ± 0.03 mm (Figure 6, *B*) at 1 month. The radius of curvature of the stromal–epithelial

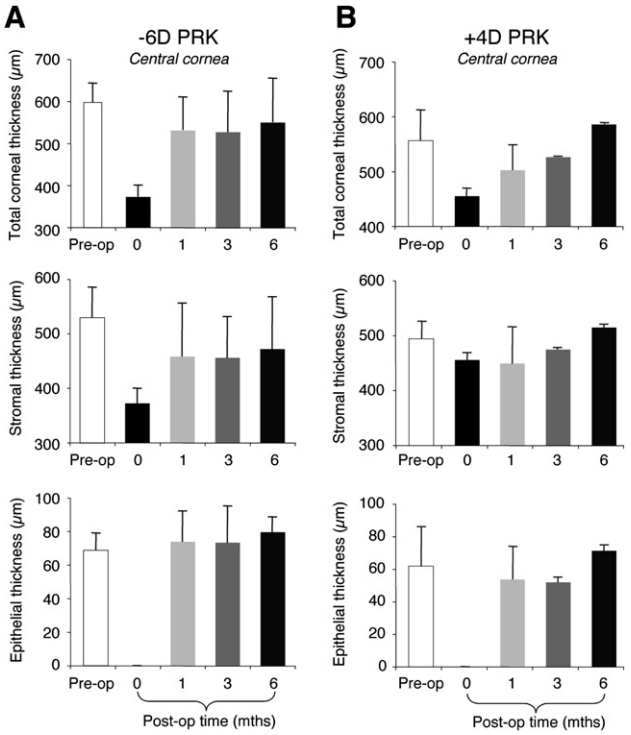

Figure 5. Effects of PRK on central thicknesses of the cat cornea, as measured using OCT. *A*: Plots of mean central thickness of the total cornea, the stromal layer, and the epithelial layer in cats that had myopic PRK over 8.0 mm OZs (n = 2). Total central corneal thickness decreased by approximately 200 μm after PRK, but returned to normal by 1 month postoperatively. Most of this increase appeared driven by stromal remodeling. Epithelial thickness decreased to 0 μm as a result of PRK but returned to normal by 1 month postoperatively, remaining at that level over the next 5 months. *B*: Plots of mean central thickness of the total cornea, the stromal layer, and the epithelial layer in cats that had hyperopic PRK over 8.0 mm OZs (n = 2). Total CCT decreased by only approximately 100 μm after PRK, and gradually returned to normal over the next 6 months. Unlike cats with myopic PRK, the remodeling of CCT in cats with hyperopic PRK appeared driven fairly equally by stromal and epithelial regrowth (values expressed as means ± SD).

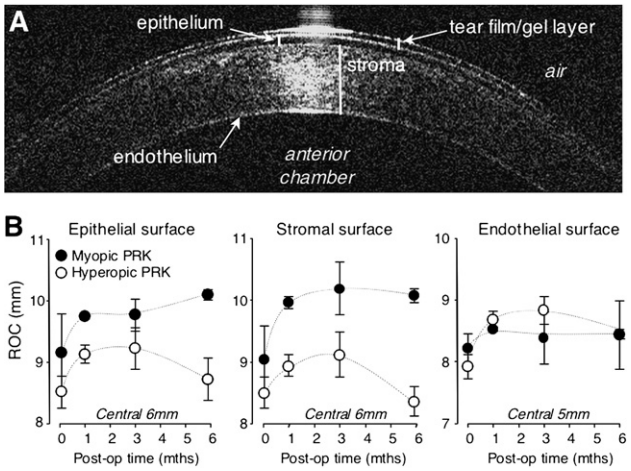

Figure 6. Effects of PRK on central radii of curvature of the cat cornea, as measured using OCT. *A*: Sample OCT image of the cat cornea illustrating the different visible layers (protective gel layer, epithelium, stroma, and endothelium), as well as the relative location of the air and anterior chamber of the eye. *B*: Plots of mean radii of curvature of the epithelial, stromal, and endothelial surfaces of the cat cornea preoperatively as well as 1, 3, and 6 months after PRK over 8.0 mm OZs. Data for cats that had myopic PRK are represented by dark gray symbols while data for cats that had hyperopic PRK are indicated by white symbols. Note that all animals had an increase in radius of curvature over the central 6.0 mm of cornea after surgery, although hyperopic PRK caused less of a flattening than myopic PRK and this flattening became a steepening by 6 months postoperatively, particularly at the epithelial and stromal surfaces. By contrast, cats with myopic PRKs exhibited a strong increase in corneal radius of curvature at 1 month after surgery and maintained this flattening throughout the postoperative period. Note also all 3 corneal surfaces exhibited some amount of flattening, including the endothelial surface, although this was not statistically significant for the latter (values expressed as means ± SD).

interface (labeled "stromal" in the Figures) also increased from a mean of 8.9 ± 0.8 mm to a mean of 9.9 ± 0.1 mm (Figure 6, *B*). In contrast, the endothelial radius of curvature changed less (mean 8.1 ± 0.4 mm preoperatively to 8.5 ± 0.1 mm 1 month postoperatively) (Figure 6, *B*). The flattening of the 2 anterior corneal surfaces was maintained over the 5 months after myopic PRKs. This paralleled the initial hyperopic shift (from preoperative to 1 month postoperative) and subsequent refractive stability (from 1 to 6 months postoperative) observed for the defocus term in cats treated with 8.0 mm OZs (Figure 4, *A*). One month after hyperopic PRK over 8.0 mm OZs, a relatively small increase in anterior, stromal, and endothelial radii of curvature was observed over the central 6.0 mm of cornea (Figure 6, *B*). These flatter corneas persisted to 3 months after hyperopic PRK; however, unlike corneas with myopic treatments, they became steeper than before surgery by 6 months after hyperopic PRK. An ANOVA showed the observed differences in the curvature changes between myopic ablations and hyperopic ablations over time were most significant at the epithelial surface and the stromal–epithelial interface ($P = .009$ and $P = .025$, respectively). The effect was not significant at the endothelial surface ($P = .365$). The most striking observation, however, was that there was no decrease in the anterior and stromal radii of curvature over the first 3 months after hyperopic PRK (Figure 6, *B*), even though the myopic shift in the defocus term in these cats (Figure 3, *A*) would predict that there should be such a change.

One month and 3 months after PRK, the mean axial length in the cat eye was 22.8 ± 0.1 mm and 22.9 ± 0.2 mm, respectively, which was not significantly different from preoperative values ($P > .05$, 2-tailed Student *t* test).

One month after PRK, whether myopic or hyperopic (no significant effect of group observed), corneal hysteresis in the cats decreased significantly from a mean of 8.4 ± 1.8 mm Hg to a mean of 4.7 ± 0.4 mm Hg. However, it recovered to normal levels over the next 5 months (Figure 7, *A*). Similarly, the mean corneal resistance factor decreased significantly from 7.0 ± 1.5 mm Hg preoperatively to 3.1 ± 1.0 mm Hg 1 month after PRK, increasing slightly over the next 5 months (Figure 7, *B*). In contrast, IOPg and IOPcc were not significantly affected by PRK, although IOPg appeared to decrease slightly after PRK relative to the preoperative values (Figure 7, *C* and *D*).

Effect of Photorefractive Keratectomy on Cat Corneal Histology

As shown in hematoxylin-stained sections (Figure 8), the normal feline cornea possesses a histological structure resembling that of other mammalian corneas examined. The cat cornea is covered by a stratified epithelium, a stroma populated by keratocytes that normally stain positive for vimentin but not α-SMA, and a single-cell layer endothelium. A thin Bowman's layer separates the epithelium from stromal keratocytes in unoperated corneas but disappears after PRK (Figure 8). Descemet's membrane is also present, separating the stroma from the endothelium (Figure 8). After PRK, hematoxylin staining showed an increased density of stromal cells under the regenerated epithelium, which persisted out to 3 months after surgery (Figure 8). At least some stromal cells that lay under the ablation epithelium appeared to be keratocytes as they stained positive for vimentin. One month after PRK, a proportion of these stromal cells also stained

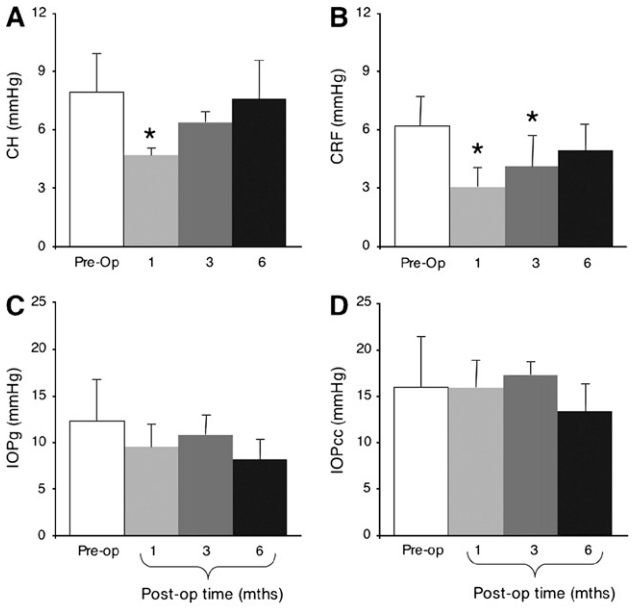

Figure 7. Effects of PRK on viscoelastic properties of the cat cornea and on IOP. Cats from all surgical groups (myopic and hyperopic PRK, over 6.0 mm and 8.0 mm OZs) were combined for this analysis. *A*: Ablated corneas exhibited a significant decrease in corneal hysteresis (CH) 1 month after PRK relative to preoperative values, but they recovered toward normal values 3 and 6 months postoperatively. *B*: The corneal resistance factor (CRF) was lowest 1 month after PRK, recovering slowly over the next 5 months so that by 6 months postoperatively, it was not significantly different from preoperative values. *C*: Corresponding histogram for IOPg shows that PRK does not significantly change IOPg in cats. *D*: Similarly, IOPcc remained unchanged after PRK (values expressed as means ± SD; * = significant difference from preoperative values at $P < .05$ level, 2-tailed Student *t* test).

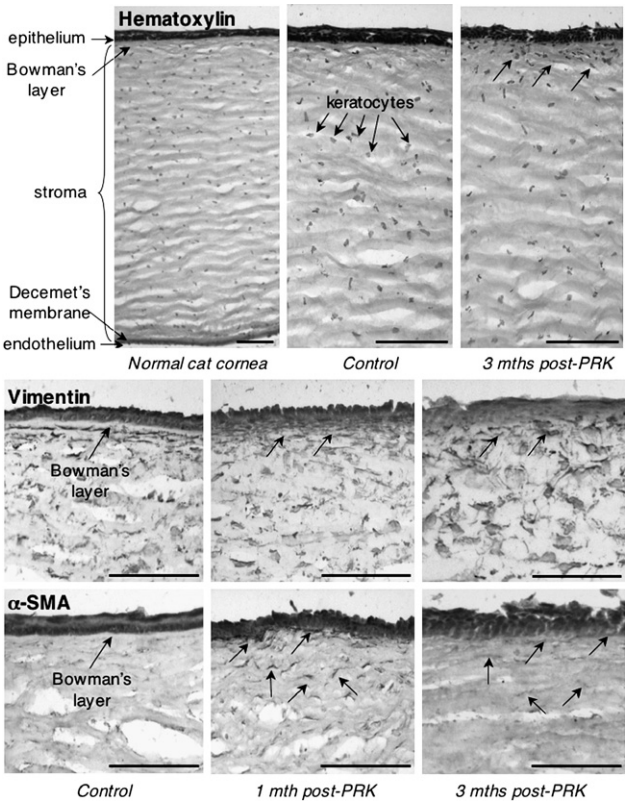

Figure 8. Histopathology of the cat cornea after PRK. Hematoxylin staining of the normal cat cornea shows histological structure consistent with that previously published and including a stratified epithelium, Bowman's layer, a stroma populated by keratocytes, a very thin Descemet's membrane, and an endothelium. Three months after PRK, the cat cornea exhibited a typical cellular response, with an increased density of stromal keratocytes immediately under the ablation epithelium (*arrows*). Vimentin immunolabeling showed a population of quiescent keratocytes in the normal cat stroma, which increases in density at 1 month and 3 months after PRK. Note the absence of a clearly demarcated Bowman's layer after PRK. The α-SMA immunostaining shows lack of stromal reactivity before PRK but increased expression in stromal keratocytes (myofibroblasts, *arrow*) under the ablation 1 month after PRK. This reactivity decreased by 3 months post-PRK, although some faintly labeled cells could still be seen in the subablation stroma (*arrow*) (bars = 100 μm).

positive for α-SMA (Figure 8, *arrow*), suggesting they were myofibroblasts. However, although the increased density of subablation keratocytes persisted out to 3 months postoperatively, there was a significant reduction in α-SMA expression under the ablation epithelium at this time point (Figure 8).

DISCUSSION

The contribution of corneal biology to the optical changes caused by laser refractive surgery is a topic of great current interest. Significant effort is being directed toward understanding what aspects of corneal biology and biomechanics are responsible for the negative optical outcomes of this procedure. Our goal here was to examine optical changes induced by PRK in a cat animal model. Although similar in gross structure and thickness, cat and human corneas differ in surface area, corneal hysteresis, the corneal resistance factor, and regenerative capacity, offering an interesting paradigm to evaluate the relative importance of these factors in refractive outcomes. However, what makes cats a particularly good animal model for our studies is that they can be trained to fixate on visual targets with the same degree of precision as humans.[11] This enabled us to measure wavefront aberrations in cats under the same conditions (ie, in the awake-fixating state) as in humans. As a result, we could monitor surgically induced changes in ocular wavefront aberrations, corneal thickness, shape, and rigidity at the same time points.

Similarities and Differences Between Normal Cat and Human Corneas

Our measurements showed cat corneas have similar total central thickness, thickness of epithelial and stromal layers, and general anatomical organization as human corneas.[16,22,35–38] In addition, we found no significant differences between cat and human IOPcc, suggesting that the cat cornea is under similar internal pressures as the human cornea. However, the surface area of cat corneas appeared significantly larger than that of human corneas. To verify this, we used published average corneal diameters[16–20] to first calculate the sagittal height of the "average" cat and human cornea as follows:

$$H = h(R) - h(0)$$

$$h(R) = \frac{C \times R^2}{1 + \sqrt{1 - (k \times C^2 \times R^2)}}$$

where H is the total height of the cornea, C = the curvature of the surface (1/radius of curvature r), R = corneal radius, measured from the center of the cornea to the corneoscleral junction, and k is conic constant, in this case a value of 1 assuming a spherical dome. The surface area of the prototypical cat and human cornea was then computed using the standard formula for the surface area of a spherical dome:

$$\text{Surface area} = 2\pi Hr$$

This gave an approximate surface area of 316 mm^2 for the average feline cornea and approximately 130 mm^2 for the average human cornea. Thus, cat corneas are approximately 2.4 times larger than human corneas, something we believe may have significant implications for refractive outcome after laser ablation (see below).

The native biomechanical properties of cat and human corneas also appeared to differ significantly. Both corneal hysteresis and the corneal resistance factor were smaller in cats than in humans preoperatively, suggesting the cat cornea is normally less rigid than the human cornea.[2] It is unlikely that this difference was a result of measurement error. Although the coefficients of variation were greater for ORA measurements in cats than in humans, these coefficients were always significantly smaller than the differences observed between cat data and human data. The greater coefficients of variation in cats are probably because unlike the humans we examined, the cats were not awake and fixating on the machine's target when measurements were collected. They were anesthetized and while their eyes were wide open, the experimenter had to estimate ocular alignment to the ORA 5 to 6 times during each measurement session. A parallax-driven error in ocular alignment is a likely cause of our large coefficient of variation in cats. Aside from this, however, the parametric data in our small sample of human subjects with regards to corneal hysteresis, the corneal resistance factor, IOP, and ocular axial length were consistent with previously published measurements[2,20,39] (Luce DA. IOVS 2006; 47:ARVO E-Abstract 2266). Because the same instruments (ORA and IOLMaster) were used in our sample of cats, we are relatively confident that our animal data are comparable to data in the literature on humans.

Low corneal rigidity, usually seen after laser refractive surgery and in keratoconus,[2,40] is thought to imply biomechanical instability and is often predictive of pathological reactions to laser refractive surgery, including the development of keratectasia.[41–43] Why normal cat corneas should have low hysteresis and corneal resistance factor remains to be determined. Perhaps the collagen fibril arrangement needed to support the greater surface area of feline corneas differs from that needed to support human corneas. Part of this difference may lie in the manner in which collagen fibrils that cover the cornea integrate with limbal

fibers. The specific nature of this arrangement is thought to be important for the maintenance of the different corneal and scleral curvatures,[24,44,45] and has been postulated to influence corneal rigidity.[24,44,45] Alternatively, the proteoglycan-collagen fibril organization, known to affect viscoelastic properties of the cornea,[46] may differ in the 2 species. Yet another possibility is that the thinner feline Bowman's membrane[23] does not stabilize its cornea to the same degree as its thicker counterpart in humans.[23]

Effects of Photorefractive Keratectomy on Feline Corneal Biometrics and Wound Healing

Despite their native differences in corneal area and rigidity, cat eyes and human eyes had many similarities in their biomechanical and cellular reaction to laser refractive surgery. "True" postoperative IOP in the cat, perhaps best represented by IOPcc (Luce DA. IOVS 2006; 47:ARVO E-Abstract 2266), was unchanged by refractive surgery, just as reported in humans[47] (Luce DA. IOVS 2006; 47:ARVO E-Abstract 2266). On the other hand, PRK significantly decreased corneal rigidity (corneal hysteresis and corneal resistance factor) in the cat, a phenomenon also reported in humans after laser refractive surgery[40] (Luce DA. IOVS 2006; 47:ARVO E-Abstract 2266). However, feline corneal hysteresis and the corneal resistance factor slowly increased between 1 month and 6 months after PRK, paralleling a gradual increase in stromal and total corneal thickness. This supports the notion that corneal rigidity is strongly influenced by wound healing and the changes in stromal and total corneal thickness that accompany this process (Luce DA. IOVS 2006; 47:ARVO E-Abstract 2266). It also illustrates the strong regenerative capacity of the cat cornea after injury, consistent with a recent report by Acosta et al.,[48] who reported strong corneal regeneration after implantation of supradescemetic keratoprostheses in cats. Corneal regrowth has also been reported in rabbits[49] but occurs to a much lesser extent in humans after PRK.[50] Indeed, corneal remodeling in the cat brought total CCT back to preoperative values by the sixth month after PRK that removed, on average, almost 100 μm of central stroma. For cats with myopic PRK, most of the rethickening occurred within the first postoperative month, with slower regrowth taking place between 1 month and 6 months after PRK. For cats with hyperopic ablations, the central stromal rethickening was much slower (and of a lesser magnitude) than in cats with myopic ablations; however, the final outcome was also a return to preoperative stromal and epithelial thicknesses by the end of the sixth postoperative month. As previously reported in humans and rabbits after PRK,[49–51] most observed corneal regrowth affected the stroma, while epithelial thickness, which returned to its preoperative levels by 1 month after PRK, remained stable thereafter. Although a detailed examination of the cellular wound-healing response to PRK in the cat was beyond the scope of this study, we did ascertain that the cat cornea's cellular reaction to PRK was largely similar to that reported in this species[7] as well as in rabbits,[6] monkeys,[52] and humans.[53–55] The stratified epithelium reformed over the ablation zone without reforming Bowman's layer. The α-SMA–positive myofibroblasts appeared and occupied the subepithelial zone under the ablation. The α-SMA reactivity was highest approximately 1 month after PRK, decreasing afterward; however, the subablation stroma remained hypercellular, at least out to 3 months after surgery.

Effects of Photorefractive Keratectomy on Feline Ocular Optics

In terms of optical reaction to refractive surgery, defocus changed in the intended direction after PRK in cats, becoming more myopic after hyperopic treatments and more hyperopic after myopic treatments. Cats also had an increase in the magnitude of HOAs up to and including the 5th-order Zernike terms. Changes in the amount and sign of spherical aberration were within the range reported after equivalent PRK in humans.[56,57] Cats also had relatively large increases in coma-type aberrations, probably because the animals were anesthetized for surgery and phenylephrine drops were used to keep their nictitating membranes retracted. These drops dilated their pupils beyond 12.0 mm in diameter, making centration of the laser ablation on the pupil difficult,[58] a phenomenon known to increase coma.[59]

One notable difference between optical outcomes in cats and humans having comparable refractive ablations over a 6.0 mm OZ was that cats achieved very little of the intended myopic and hyperopic refractive changes (37% and 20%, respectively). Because cat axial lengths did not change significantly after PRK, rapid postoperative emmetropization was not likely responsible for the severe undercorrections. The IOLMaster we used can measure axial lengths ranging from 14.0 to 40.0 mm with a resolution of ± 0.01 mm. Reproducibility of the device is excellent, with a standard deviation of ± 0.03 mm in human eyes. Taking $1/f$, where f is the axial (focal) length of the eye, approximately 0.5 mm of axial length change would be needed to induce 1.0 D of power change in the cat eye. This was larger than the standard deviation of our axial length measurements and was never observed.

One factor known to significantly benefit refractive outcome is a larger OZ.[60,61] Given the larger area of cat corneas versus human corneas, we hypothesized

that our undercorrections with 6.0 mm OZs could be the result of the proportionately smaller surface area this OZ covers in the cat eye. Indeed, a 6.0 mm OZ ablates approximately 20% of the average human corneal surface area but only 9% of the average cat corneal area. Increasing cat OZs to 8.0 mm (approximately 20% of the cat's total corneal surface area) achieved 75% and 105% of our intended myopic corrections and hyperopic corrections, respectively. The amount of HOAs induced by 8.0 mm OZs relative to the total amount of monochromatic aberrations was also smaller than for 6.0 mm OZs. That a larger OZ should be advantageous for refractive outcomes has been reported in humans[62–65] and may be the result of a combination of factors involving a different biomechanical reaction of the cornea to a larger, deeper cut as well and differences in the wound-healing response.

Finally, consistent with the long-term stability previously reported for comparable refractive ablations (ie, 6.0 D myopic PRK or 4.0 D hyperopic PRK over 6.0 mm OZs) performed in humans,[66,67] no significant regression of the achieved defocus or higher-order RMS change was observed between 1 month and 6 months after PRK in the cat, although both defocus and higher-order RMS appeared more variable after hyperopic than myopic ablations. The relative refractive stability in the cat after PRK occurred in the presence of significant postoperative central stromal and epithelial remodeling, which, as mentioned earlier, returned CCT to normal levels by the sixth month after PRK. When stromal remodeling was reported in rabbits after PRK,[49] it was always assumed (although not proven) to accompany or cause refractive regression. This is because in humans, the relatively small amount of stromal thickening (approximately 8% per year) that occurs after PRK is well correlated with refractive regression.[50] Our findings in cats with PRK suggest that the phenomenon of stromal thickening in cats and rabbits compared with humans may in fact be very different. Indeed, one should probably not assume regression of optical refraction just because CCT returns to normal after surgery, especially in species that exhibit an aggressive stromal wound-healing reaction. Perhaps in cats, the corneal regrowth occurs in such a way as to preserve the new surface profile imparted by the laser ablation. In fact, our observation that anterior (epithelial surface and stromal–epithelial interface) radii of curvature increased and then remained stable in cats between 1 month and 6 months after myopic PRK supports this hypothesis. What is not so easy to reconcile is our observation of a slight increase in anterior corneal radii of curvature after hyperopic PRK in the cat at the first and third postoperative months, despite a significant myopic shift in the defocus term at the same time points. One potential explanation for this contradictory result is our use of best-fit spheres to estimate the radii of curvature of the markedly nonspherical epithelial and stromal surfaces after hyperopic PRK. Further refinement of our surface-fitting algorithm is necessary to resolve this issue.

CONCLUSIONS

The present study describes results in a cat animal model of human PRK in which it was possible to perform measurements of corneal biology, biomechanics, and optical quality at the same time points. Using this model, we highlighted a particularly important role of ablation OZ relative to the total corneal area for attaining a given refractive change in corneas with natively low hysteresis and the corneal resistance factor. In addition, we showed that stromal and epithelial remodeling are not necessarily associated with refractive regression in the cat, a species that like the rabbit, exhibits aggressive wound healing after laser refractive surgery. The native differences in corneal properties and wound healing that exist between cats and humans reveal a rather more complex relationship between corneal biology, biomechanics, and ocular optics than previously envisaged. Defining and understanding this relationship should help us develop more effective therapeutic manipulations to optimize the optical outcomes of corneal surgeries in humans.

REFERENCES

1. Moreno-Barriuso E, Merayo Lloves J, Marcos S, et al. Ocular aberrations before and after myopic corneal refractive surgery: LASIK-induced changes measured with laser ray tracing. Invest Ophthalmol Vis Sci 2001; 42:1396–1403
2. Luce DA. Determining in vivo biomechanical properties of the cornea with an ocular response analyzer. J Cataract Refract Surg 2005; 31:156–162
3. Roberts C. Biomechanics of the cornea and wavefront-guided laser refractive surgery. J Refract Surg 2002; 18: S589–S592
4. Roberts C, Dupps WJ Jr. Corneal biomechanics and their role in corneal ablative procedures. In: MacRae SM, Krueger RR, Applegate RA, eds, Customized Corneal Ablation; the Quest for SuperVision. Thorofare, NJ, Slack, 2001; 109–131
5. Fini ME. Keratocyte and fibroblast phenotypes in the repairing cornea. Prog Retin Eye Res 1999; 18:529–551
6. Jester JV, Petroll WM, Cavanagh HD. Corneal stromal wound healing in refractive surgery: the role of myofibroblasts. Prog Retin Eye Res 1999; 18:311–356
7. Telfair WB, Bekker C, Hoffman HJ, et al. Healing after photorefractive keratectomy in cat eyes with a scanning mid-infrared Nd:YAG pumped optical parametric oscillator laser. J Refract Surg 2000; 16:32–39
8. Wilson SE. Analysis of the keratocyte apoptosis, keratocyte proliferation, and myofibroblast transformation responses after photorefractive keratectomy and laser in situ keratomileusis. Trans Am Ophthalmol Soc 2002; 100:411–433; available at: http://

www.aosonline.org/2001xactions.html. Accessed March 9, 2007
9. Wilson SE, Liu JJ, Mohan RR. Stromal-epithelial interactions in the cornea. Prog Retin Eye Res 1999; 18:293–309
10. Koh S, Maeda N, Kuroda T, et al. Effect of tear film break-up on higher-order aberrations measured with wavefront sensor. Am J Ophthalmol 2002; 134:115–117
11. Huxlin KR, Pasternak T. Training-induced recovery of visual motion perception after extrastriate cortical damage in the adult cat. Cerebral Cortex 2004; 14:81–90
12. Pasternak T, Maunsell JH. Spatiotemporal sensitivity following lesions of area 18 in the cat. J Neurosci 1992; 12:4521–4529
13. Pasternak T, Tompkins J, Olson CR. The role of striate cortex in visual function of the cat. J Neurosci 1995; 15:1940–1950
14. Pasternak T, Horn K. Spatial vision of the cat: variation with eccentricity. Vis Neurosci 1991; 6:151–158
15. Huxlin KR, Yoon G, Nagy L, et al. Monochromatic ocular wavefront aberrations in the awake-behaving cat. Vision Res 2004; 44:2159–2169
16. Carrington SD, Woodward EG. Corneal thickness and diameter in the domestic cat. Ophthalmic Physiol Opt 1986; 6: 385–389
17. Rüfer F, Schröder A, Erb C. White-to-white corneal diameter normal values in healthy humans obtained with the Orbscan II topography system. Cornea 2005; 24:259–261
18. Vakkur GJ, Bishop PO. The schematic eye in the cat. Vision Res 1963; 3:375–381
19. Hughes A. A supplement to the cat schematic eye. Vision Res 1976; 16:149–154
20. Hughes A. The topography of vision in mammals of contrasting life style: Comparative optics and retinal organisation. In: Crescitelli F, eds, The Visual System In Vertebrates. Volume VII/5 of Handbook of Sensory Physiology. Berlin, Springer Verlag, 1977; 613–756
21. Jester JV, Barry PA, Lind GJ, et al. Corneal keratocytes: in situ and in vitro organization of cytoskeletal contractile proteins. Invest Ophthalmol Vis Sci 1994; 35:730–743
22. Li HF, Petroll WM, Møller-Pedersen T, et al. Epithelial and corneal thickness measurements by in vivo confocal microscopy through focusing (CMTF). Curr Eye Res 1997; 16:214–221
23. Hayashi S, Osawa T, Tohyama K. Comparative observations on corneas, with special reference to Bowman's layer and Descemet's membrane in mammals and amphibians. J Morphol 2002; 254:247–258
24. Meek KM, Boote C. The organization of collagen in the corneal stroma. Exp Eye Res 2004; 78:503–512
25. Boote C, Hayes S, Abahussin M, Meek KM. Mapping collagen organization in the human cornea: left and right eyes are structurally distinct. Invest Ophthalmol Vis Sci 2006; 47:901–908
26. Jester JV, Petroll WM, Feng W, et al. Radial keratotomy. 1. The wound healing process and measurement of incisional gape in two animal models using in vivo confocal microscopy. Invest Ophthalmol Vis Sci 1992; 33:3255–3270
27. Courville CB, Smolek MK, Klyce SD. Contribution of the ocular surface to visual optics. Exp Eye Res 2004; 78:417–425
28. Marcos S, Barbero S, Llorente L, Merayo-Lloves J. Optical response to LASIK surgery for myopia from total and corneal aberration measurements. Invest Ophthalmol Vis Sci 2001; 42: 3349–3356
29. Llorente L, Barbero S, Merayo J, Marcos S. Total and corneal optical aberrations induced by laser in situ keratomileusis for hyperopia. J Refract Surg 2004; 20:203–216
30. Petroll WM, Cavanagh HD, Jester JV. Assessment of stress fiber orientation during healing of radial keratotomy wounds using confocal microscopy. Scanning 1998; 20:74–82
31. Telfair WB, Bekker C, Hoffman HJ, et al. Histological comparison of corneal ablation with ER:YAG laser, Nd:YAG optical parametric oscillator, and excimer laser. J Refract Surg 2000; 16: 40–50
32. Thibos LN, Applegate RA, Schwiegerling JT, Webb R. Standards for reporting the optical aberrations of eyes; VSIA Standards Taskforce Members. In: MacRae SM, Krueger RR, Applegate RA, eds, Customized Corneal Ablation; the Quest for SuperVision. Thorofare NJ, Slack, 2001; 348–361
33. Radhakrishnan S, Rollins AM, Roth JE, et al. Real-time optical coherence tomography of the anterior segment at 1310 nm. Arch Ophthalmol 2001; 119:1179–1185
34. Wang J, Thomas J, Cox I, Rollins A. Noncontact measurements of central corneal epithelial and flap thickness after laser in situ keratomileusis. Invest Ophthalmol Vis Sci 2004; 45: 1812–1816
35. Reinstein DZ, Silverman RH, Rondeau MJ, Coleman DJ. Epithelial and corneal thickness measurements by high-frequency ultrasound digital signal processing. Ophthalmology 1994; 101:140–146
36. Phillips LJ, Cakanac CJ, Eger MW, Lilly ME. Central corneal thickness and measured IOP: a clinical study. Optometry 2003; 74:218–225
37. Barkana Y, Gerber Y, Elbaz U, et al. Central corneal thickness measurement with the Pentacam Scheimpflug system, optical low-coherence reflectometry pachymeter, and ultrasound pachymetry. J Cataract Refract Surg 2005; 31:1729–1735
38. Lackner B, Schmidinger G, Pieh S, et al. Repeatability and reproducibility of central corneal thickness measurement with Pentacam, Orbscan, and ultrasound. Optom Vis Sci 2005; 82: 892–899
39. Sheng H, Bottjer CA, Bullimore MA. Ocular component measurement using the Zeiss IOLMaster. Optom Vis Sci 2004; 81: 27–34
40. Hjortdal JØ, Møller-Pedersen T, Ivarsen A, Ehlers N. Corneal power, thickness, and stiffness: results of a prospective randomized controlled trial of PRK and LASIK for myopia. J Cataract Refract Surg 2005; 31:21–29
41. Comaish IF, Lawless MA. Progressive post-LASIK keratectasia; biomechanical instability or chronic disease process? J Cataract Refract Surg 2002; 28:2206–2213
42. Guirao A. Theoretical elastic response of the cornea to refractive surgery: risk factors for keratectasia. J Refract Surg 2005; 21:176–185
43. Dupps WJ Jr. Biomechanical modeling of corneal ectasia. J Refract Surg 2005; 21:186–190; errata 2007; 22:9
44. Maurice DM. The cornea and sclera. In: Davson H, ed, The Eye, 3rd ed. Orlando, FL, Academic Press, 1984; vol 1B:1–158
45. Boote C, Dennis S, Meek KM. Spatial mapping of collagen fibril organisation in primate cornea—an X-ray diffraction investigation. J Struct Bio 2004; 146:359–367
46. Müller LJ, Pels E, Schurmans LRHM, Vrensen GFJM. A new three-dimensional model of the organization of proteoglycans and collagen fibrils in the human cornea. Exp Eye Res 2004; 78:493–501
47. Dupps WJ Jr, Wilson SE. Biomechanics and wound healing in the cornea. Exp Eye Res 2006; 83:709–720
48. Acosta AC, Espana EM, Stoiber J, et al. Corneal stroma regeneration in felines after supradescemetic keratoprosthesis implantation. Cornea 2006; 25:830–838
49. Møller-Pedersen T, Li HF, Petroll WM, et al. Confocal microscopic characterization of wound repair after photorefractive keratectomy. Invest Ophthalmol Vis Sci 1998; 39:487–501
50. Møller-Pedersen T, Cavanagh HD, Petroll WM, Jester JV. Stromal wound healing explains refractive instability and haze

development after photorefractive keratectomy; a 1-year confocal microscopic study. Ophthalmology 2000; 107:1235–1245
51. Møller-Pedersen T, Cavanagh HD, Petroll WM, Jester JV. Neutralizing antibody to TGFβ modulates stromal fibrosis but not regression of photoablative effect following PRK. Curr Eye Res 1998; 17:736–747
52. Fantes FE, Hanna KD, Waring GO III, et al. Wound healing after excimer laser keratomileusis (photorefractive keratectomy) in monkeys. Arch Ophthalmol 1990; 108:665–675
53. Dawson DG, Edelhauser HF, Grossniklaus HE. Long-term histopathologic findings in human corneal wounds after refractive surgical procedures. Am J Ophthalmol 2005; 139:168–178
54. Amano S, Shimizu K, Tsubota K. Corneal epithelial changes after excimer laser photorefractive keratectomy. Am J Ophthalmol 1993; 115:441–443
55. Lohmann CP, Patmore A, O'Brart D, et al. Regression and wound healing after excimer laser PRK: a histopathological study on human corneas. Eur J Ophthalmol 1997; 7:130–138
56. Seiler T, Kaemmerer M, Mierdel P, Krinke H-E. Ocular optical aberrations after photorefractive keratectomy for myopia and myopic astigmatism. Arch Ophthalmol 2000; 118:17–21
57. Mierdel P, Kaemmerer M, Krinke H-E, Seiler T. Effects of photorefractive keratectomy and cataract surgery on ocular optical errors of high order. Graefes Arch Clin Exp Ophthalmol 1999; 237:725–729
58. Porter J, Yoon G, Lozano D, et al. Aberrations induced in wavefront-guided laser refractive surgery due to shifts between natural and dilated pupil center locations. J Cataract Refract Surg 2006; 32:21–32
59. Mrochen M, Kaemmerer M, Mierdel P, Seiler T. Increased higher-order optical aberrations after laser refractive surgery; a problem of subclinical decentration. J Cataract Refract Surg 2001; 27:362–369
60. O'Brart DPS, Gartry DS, Lohmann CP, et al. Excimer laser photorefractive keratectomy for myopia: comparison of 4.00- and 5.00-millimeter ablation zones. J Refract Corneal Surg 1994; 10:87–94
61. O'Brart DPS, Corbett MC, Lohmann CP, et al. The effects of ablation diameter on the outcome of excimer laser photorefractive keratectomy; a prospective, randomized, double-blind study. Arch Ophthalmol 1995; 113:438–443
62. Mok KH, Lee VW-H. Effect of optical zone ablation diameter on LASIK-induced higher order optical aberrations. J Refract Surg 2005; 21:141–143
63. Bühren J, Kühne C, Kohnen T. Influence of pupil and optical zone diameter on higher-order aberrations after wavefront-guided myopic LASIK. J Cataract Refract Surg 2005; 31: 2272–2280
64. Endl MJ, Martinez CE, Klyce SD, et al. Effect of larger ablation zone and transition zone on corneal optical aberrations after photorefractive keratectomy. Arch Ophthalmol 2001; 119: 1159–1164
65. Seo KY, Lee JB, Kang JJ, et al. Comparison of higher-order aberrations after LASEK with a 6.0 mm ablation zone and a 6.5 mm ablation zone with blend zone. J Cataract Refract Surg 2004; 30:653–657
66. O'Brart DPS, Patsoura E, Jaycock P, et al. Excimer laser photorefractive keratectomy for hyperopia: 7.5-year follow-up. J Cataract Refract Surg 2005; 31:1104–1113
67. Rajan MS, Jaycock P, O'Brart D, et al. A long-term study of photorefractive keratectomy; 12-year follow-up. Ophthalmology 2004; 111:1813–1824

First author:
Lana J. Nagy

Department of Ophthalmology, University of Rochester, Rochester, New York, USA